JOURNAL OF PROPULSION AND POWER
Vol. 25, No. 2, March–April 2009

Experiments on Electrically Controlled Flameholding on a Plane Wall in Supersonic Airflow

Sergey Leonov* and Dmitry Yarantsev†
Russian Academy of Sciences, 125412, Moscow, Russia
and
Campbell Carter‡
U.S. Air Force Research Laboratory, Wright–Patterson Air Force Base, Ohio 45433

DOI: 10.2514/1.38002

We describe experiments on gaseous fuel ignition and flameholding controlled by an electrical discharge in high-speed airflow. The geometrical configuration does not include any mechanical or physical flameholder. The fuel is nonpremixed and injected directly into the air crossflow from the combustor bottom wall. A multi-electrode, nonuniform transversal electrical discharge is excited, also on the bottom wall, between flush-mounted electrodes. The initial gas temperature is lower than the value for autoignition of hydrogen and ethylene. Results are presented for a wide range of fuel mass flow rate and discharge power deposited into the flow. This coupling between the discharge and the flow presents a new type of flameholder over a plane wall for a high-speed combustor.

Nomenclature

G = mass flow rate
M = Mach number
P = gas pressure
T = gas temperature
W = discharge power (delivered)
X = streamwise location, measured from the location of the row of electrodes
Y = height above the bottom floor

Introduction

SOME key problems related to supersonic combustion and flame stabilization are difficult to solve for the practical implementation of such a technology, especially in the case of nonoptimal conditions and the use of hydrocarbon fuel. Among them are global ignition at low temperature and flame stabilization in a predefined combustor location (which may not be the optimum location for combustion). Plasma-based methods of combustion management are now considered promising tools in this field.

Several reviews and important works have been published recently [1–22]. Based in part on these publications, we believe the efforts, with few exceptions, can be divided into the following categories: 1) simulations of nonequilibrium kinetics of combustion; 2) basic experiments on plasma-chemical kinetics; 3) low-speed flame stabilization experiments employing a nonequilibrium discharge; 4) application of "plasma torches"; 5) high-speed ignition and flameholding experiments; and, 6) mixing experiments. Obviously the list of references does not cover the entire field. The approach of this work is to devise an experiment of practical interest for supersonic combustion; it includes the use of supersonic flow, air mass flow rate up to $G_{\text{air}} = 1$ kg/s, a nonpremixed fuel–air composition, and no physical flameholding devices within the flowpath.

Received 28 April 2008; revision received 16 October 2008; accepted for publication 16 October 2008.

*Head of Laboratory, Joint Institute for High Temperatures. Associate Fellow AIAA.
†Ph.D. Student, Research Staff, Joint Institute for High Temperatures.
‡Principal Aerospace Engineer. Associate Fellow AIAA.

Several mechanisms of the effect of plasma on flow structure, ignition, and combustion processes might be listed as follows: 1) fast local ohmic heating of the medium; 2) nonequilibrium excitation and dissociation of air and fuel molecules due to electron collisions and UV radiation; 3) momentum transfer in electric and magnetic fields; and, 4) shock/instability generation. In different situations the significance of each of these can be varied. In some cases an amplification of the effect due to mutual impact is critically important, as is observed in this work, where flow-structure control by electrical discharge and gas excitation work together for ignition and stabilization of a high-speed flame.

Of course, heating of the medium by the discharge leads to an increase in the rate of the chemical reactions, not only in the vicinity of the discharge but also downstream. Furthermore, the discharge can induce flow separation at sufficiently high levels of power deposition [23]. In this way one can create a zone with favorable conditions for combustion with increased residence time, improved rates of mixing, and increased temperature. This idea was first published in [23]. Also, fuel–air reaction rates are increased due to the formation of radicals and atomic species through excitation by electrons in the electric field and by more complex processes. Thus, deposition of active particles may also reduce the level of required external power. Another benefit of this scheme is that local shock waves, generated by the obstruction imposed by the discharges, can improve the mixing process and can initiate chemical reactions due to gas heating at the shock front.

Based on both theoretical and experimental studies, it appears that nonequilibrium and nonuniform discharge operation modes provide more flexibility in implementation and, very possibly, higher performance per unit power or energy. Nonequilibrium power deposition into the gas leads to the creation of species possessing higher reactivity in comparison with those found at equilibrium conditions. It is important also that the plasma is generated in situ, just in the place of fuel–oxidizer interaction, to diminish the effect of fast relaxation and/or mixing with the surrounding air. A possible method to reduce the power consumption is to treat only a part of the gas volume with nonuniform plasma. A preferable structure may look similar to a geometrically adjusted *grate*; here, a flamefront propagates the distance between separate plasma filaments faster than it can be blown out. An additional requirement is that a reasonable technical solution be a practical one too. The experimental approach described herein is to design and configure a nonequilibrium, spatially nonuniform discharge that can be practically implemented.

In [24] we have tested the method to improve supersonic combustor performance, which is based on the generation of

plasma-induced local unsteady separation. The artificial plasma-induced zones of the flow separation can be applied instead of mechanical devices such as a ramp or a cavity, especially under nonoptimal conditions (e.g., low gas temperature and static pressure) that will not produce autoignition, or unsteady operational modes of the combustor. The flame stabilization regimes could occur at a relatively low level of extra power deposition. In this paper the results are presented for a wider range of parameters: two fuels—hydrogen, H_2, and ethylene, C_2H_4—and different air temperatures. Furthermore, the diagnostic methods have been improved significantly over those previously used by our group.

Test Description

The experimental facility PWT-50H is used for the test of ethylene and hydrogen ignition and flameholding by an electrical discharge over a plane wall within a high-speed duct. The facility is a short-duration blowdown wind tunnel with test section dimensions of $Y \times Z = 72 \times 60$ mm. It is equipped with an air heater employing plasma-assisted combustion of ethylene (50 kW of electrical power plus up to 650 kW of thermal power due to ethylene combustion). In the described tests, the stagnation temperature of air was either $T_0 = 300$, 500, or 650 K. A more detailed description of the facility PWT-50H is presented in [24,25].

Our experiments are characterized by the following parameters: Mach number of the undisturbed flow $M = 1.9$–2; static pressure $P_{st} = 100$–150 torr; typical airflow rate $G_{air} = 0.6$–0.9 kg/s; typical fuel mass flow rate $G_{fuel} = 0.1$–6 g/s; discharge power $W_{pl} = 1$–10 kW; and, test duration $t < 0.5$ s. The facility is equipped with pressure transducers (16 points accurate within 10 torr), a schlieren system, a schlieren/streak-camera system for high-speed line imaging, devices for optical and spectroscopic observations, current-voltage sensors, etc. The exhaust-gas concentrations of O_2, CO_2, NO, CO, and C_xH_y were also measured to infer combustion efficiency.

A schematic of the experimental configuration is shown in Fig. 1. The location of the line of electrodes corresponds to $X = 0$. An important aspect of the design is the location for fuel injection. Previously, two principal fuel injection schemes were tested for a free plasma mode and for a plasma torch: upstream of the discharge and downstream of the discharge. The latter scheme demonstrated a significant benefit and is thus used here. As seen in Fig. 1, the bottom wall is inclined ($\alpha = 20$ deg), starting at $X = 50$ mm, to mitigate thermal choking of the duct upon combustion heat release. The final duct height was at the maximum value for the facility: $Y = 72$ mm. The top and side walls are simple flat plates; the side walls are equipped with windows for optical measurements.

The electrical discharge was excited *transversally* with a scheme that included electrodes arranged across the duct span in a pattern of anode–cathode–anode–cathode–anode; the electrodes are embedded in a refractory ceramic block that provides electrical insulation. Three different designs were used, with three, five, or seven electrodes. The power supply possesses a steep falling voltage-current characteristic with voltage amplitude at zero current (at initiation) of about 5 kV. A short time after initiation, the discharge has an appearance similar to that shown in Fig. 2 (here, with the 7-electrode configuration). One can see that the fuel acts to lift the discharge *loops* from the tunnel bottom floor (bottom image). Furthermore, the arc loops are seen to stretch downstream, following the flow [26]. In general, the loops will elongate, from a direct anode–cathode path, as the conductive path is convected downstream, and the maximum length of the loops is governed by the combination of maximum power supply voltage and interelectrode gap. This maximum length of the discharge filament and the gas velocity define the effective frequency of the discharge oscillations. Power release regulation was realized by the discharge current variation in a range $I_{pl} = 1$–10 A. If the current is increased by a factor of 10, the voltage is decreased, but only by a factor of 5, and as a result the power is increased by about 2 times. Such a method leads to some variation in the *reduced electric field*, which may be important for understanding of some features of the interaction. Note that the reduced electric field is defined as the electric field divided by the gas number density and is a key parameter in determining the mean electron energy and the departure from equilibrium (typically quantified by determining the degree to which the electron temperature is greater than the gas temperature). At low current the discharge is unstable, whereas at high current, electrode erosion is significant. Temperature measurements based on optical emission spectroscopy of the N_2 second-positive system (i.e., $C^3\Pi \leftarrow B^3\Pi$ emission) yield a rotational temperature of $T_g = 3500 \pm 300$ K, independent of the power release from the discharge under conditions of this experiment. Typical oscillograms of two regimes are shown in Fig. 3. The instantaneous amplitude of the discharge power can vary by a factor 2 or more; however, the average power W_{av}, measured by integrating the power waveform, does not vary more than ± 0.2 kW from one run to the next.

The fuel was injected through five circular (diameter = 3.5 mm) orifices all in a row across the span and inclined at 25 deg from the normal in the upstream direction. The row of injectors is 15 mm downstream from the row of electrodes, just downstream of the ceramic electrode block; each injector is in line with an electrode in the configuration that includes five electrodes. The fuel mass flow rate was balanced between the orifices using a fuel plenum. Fuel injection was started before the discharge initiation and was switched off after completion of the discharge. Typically, the fuel injection continued 10–20 ms after the discharge to observe whether the flame was held or extinguished.

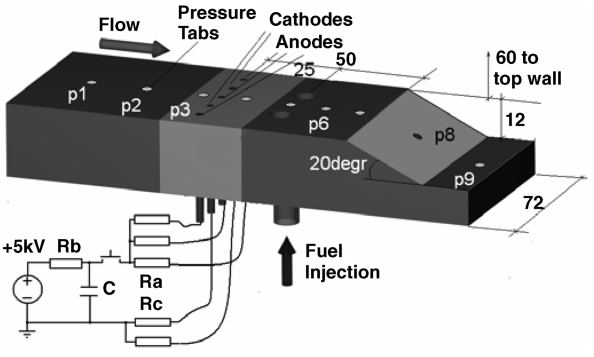

Fig. 1 Experimental schematic of the combustor bottom wall and the test arrangement.

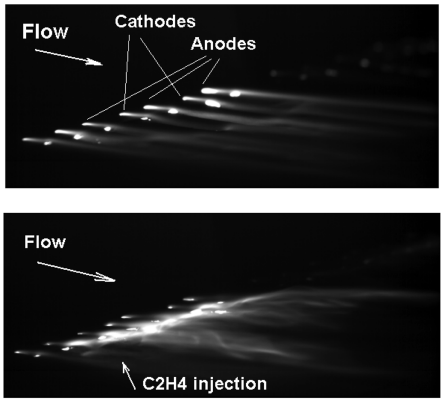

Fig. 2 Discharge photographs in a M-2 flow without fuel (top) and with ethylene injection (bottom) through five orifices. The configuration with seven electrodes is being used. Exposure time is 30 μs.

Experimental Results

A main criterion for the detection of an effect of the discharge is a rise of the static pressure within the combustion zone. The fuel ignition and flameholding were obtained experimentally with both hydrogen and ethylene fueling of the duct. Primary ignition took place behind the inclination (no separation initially). Subsequently, a flamefront propagated upstream toward the discharge location and

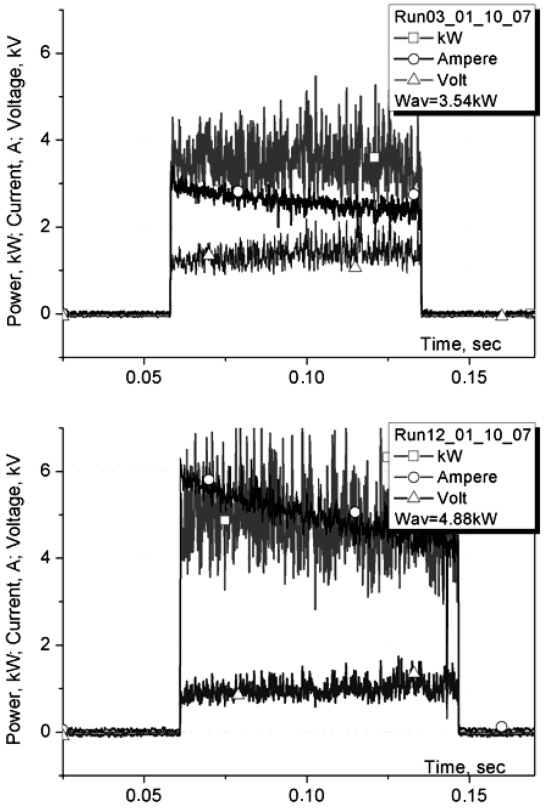

Fig. 3 Typical oscillograms for high-voltage and high-current modes of the discharge operation.

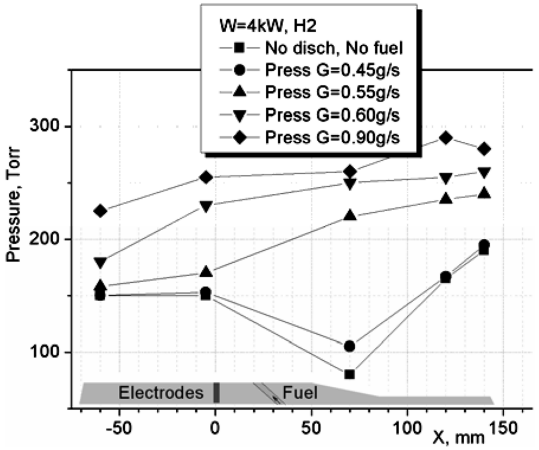

Fig. 5 Static pressure distributions for varying hydrogen flow rates at constant discharge power.

stabilized at a location that depended on fuel mass flow rate and discharge power. The data below illustrate details of plasma–fuel–flow interaction: schlieren images are shown in Fig. 4 and pressure distributions at various hydrogen flow rates are shown in Fig. 5. In the range of $G_{H2} = 0.4$–0.6 g/s, the flame position is sensitive to the fuel flow rate and discharge power. Two characteristic points were chosen as the most representative: $P3$—static pressure just upstream of the electrodes, and $P8$—static pressure at the midpoint of the inclined plane. The graphs in Fig. 6 show the dependence of pressure on the fuel flow rate and the discharge power. The same data are presented in Fig. 7 for ethylene at $W_{pl} \geq 4$ kW, when the combustion is detected. It is clearly seen that the ethylene is more difficult to ignite, requiring greater discharge power. Furthermore, it should be noted that pressure distributions were repeatable, and the end result thus predictable, not varying by more than 10% from run to run. Of course, near the power threshold for ignition, conditions were quite unstable. Instability was also observed at large fuel flow rates, and accordingly combustion completeness is observed to decrease.

The analysis of experimental data has shown that the total power W_{pl} deposited is a principal parameter. At the same time, there is some apparent influence of the power density and of the departure from equilibrium. The influence of power density was revealed by the number of electrodes switched on (recall that there are configurations with 3, 5, and 7 electrodes). Reducing the number of

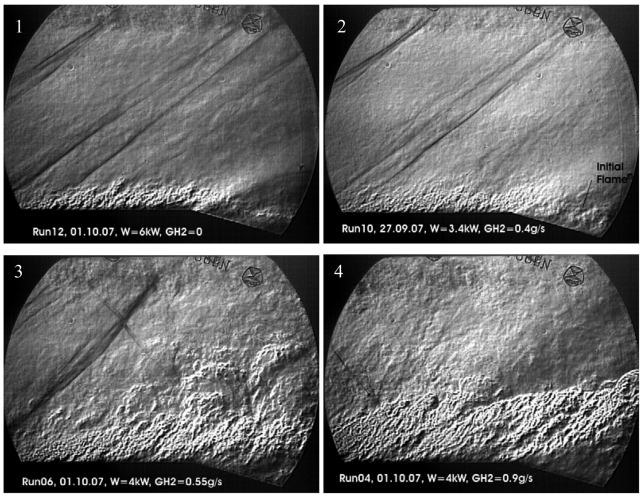

Fig. 4 Schlieren pictures in four cases: 1) no combustion (effect of discharge at $W_{pl} = 6$ kW); 2) moderate fuel flow rate and small discharge power (flamefront located behind inclination); 3) "optimal" flameholding (no choking, intense combustion); 4) transfer to $M < 1$ mode. For the scale: window diameter is 100 mm.

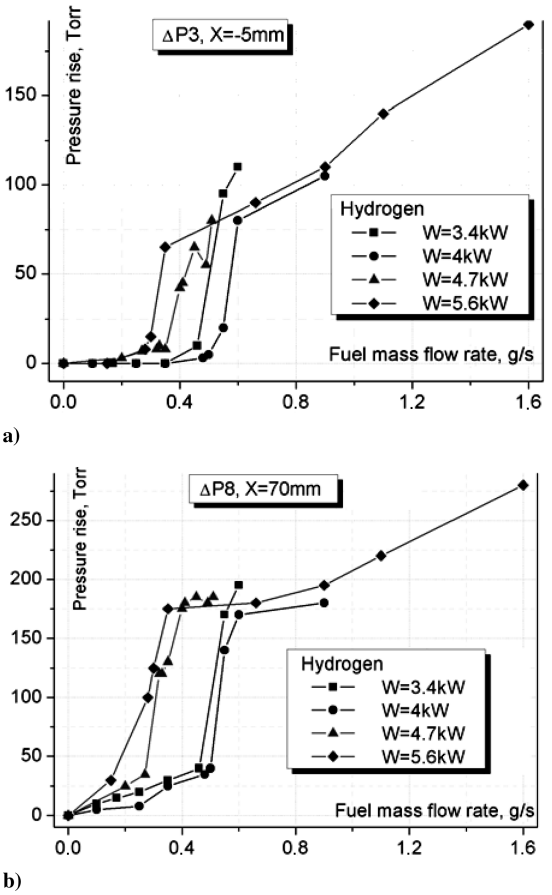

Fig. 6 Static pressure vs hydrogen flow rate at various discharge powers (3.4–5.6 kW). Top: upstream of the discharge location (P3). Bottom: at the wedge midpoint (P8).

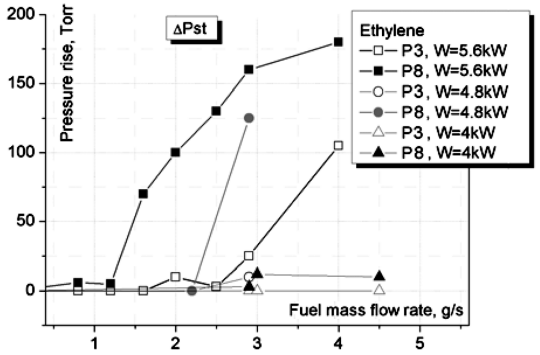

Fig. 7 Static pressure vs ethylene flow rate at various discharge powers (4–5.6 kW) upstream of the discharge location (P3) and at the wedge midpoint (P8).

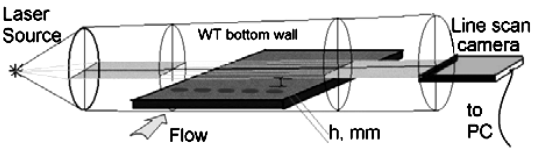

Fig. 8 Scheme of schlieren-streak visualization.

electrodes to 3 led to some decrease in the power threshold of ignition. However, the penalty of reducing the number of electrodes is that the flame appears to be more 3-D in character (i.e., less uniform across the duct). One interesting result with hydrogen fueling is that the performance, based on the pressure rise (Fig. 6), using $W_{pl} = 3.4$ kW is somewhat better than that with $W_{pl} = 4$ kW. Although the reasons for this are not fully clear, one observation that can be made is that the reduced electric field, and thus the departure from equilibrium, is higher with the lower power discharge. With regard to

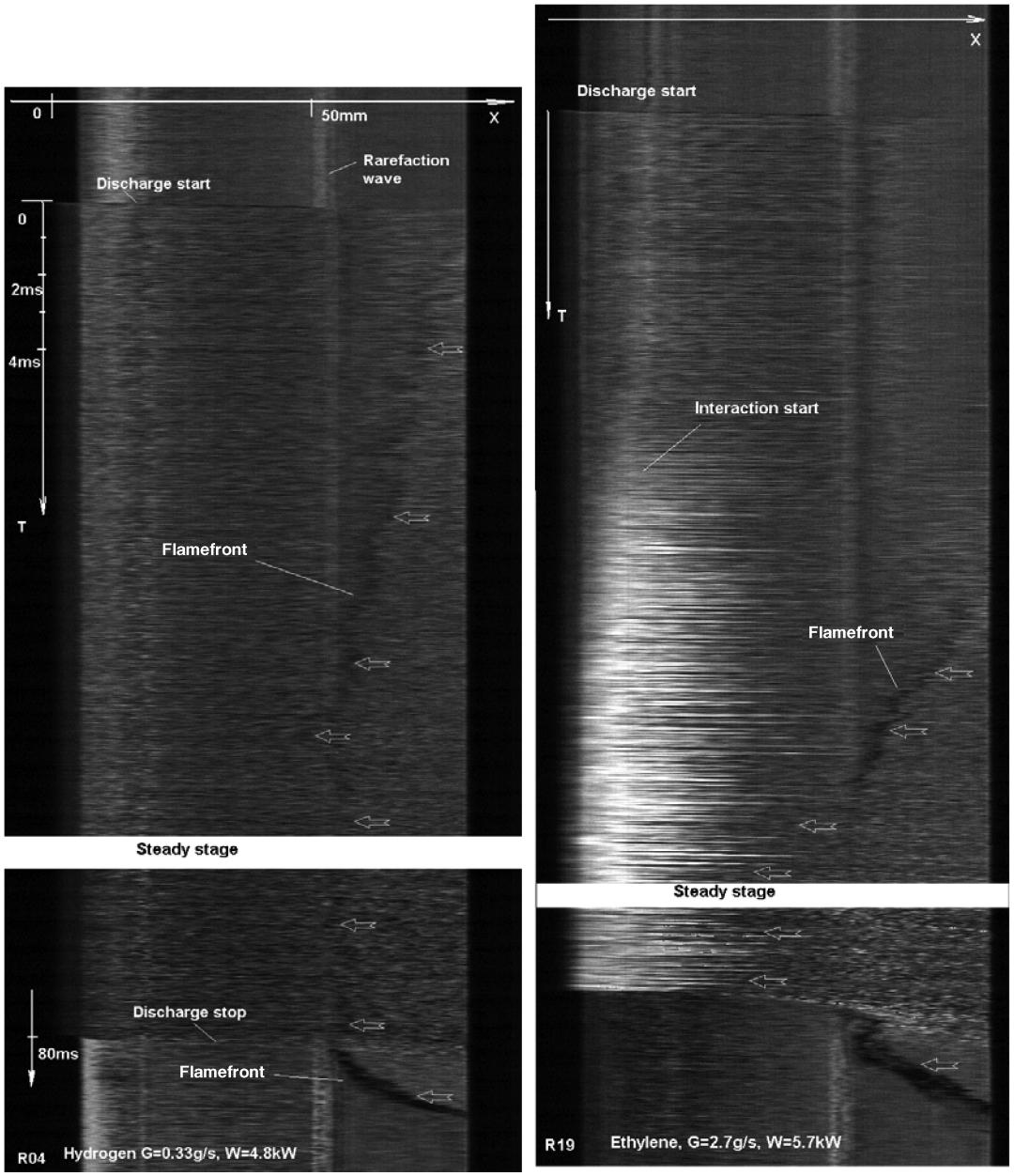

Hydrogen Fueling **Ethylene Fueling**

Fig. 9 Samples of schlieren-streak records (2-D images of downstream distance × time) for fueling with hydrogen and ethylene. In the case of hydrogen fueling (left), $G = 0.33$ g/s and $W_{pl} = 4.8$ kW; in the case of ethylene fueling (right), $G = 2.7$ g/s and $W_{pl} = 5.7$ kW. Arrows point to the flamefront position.

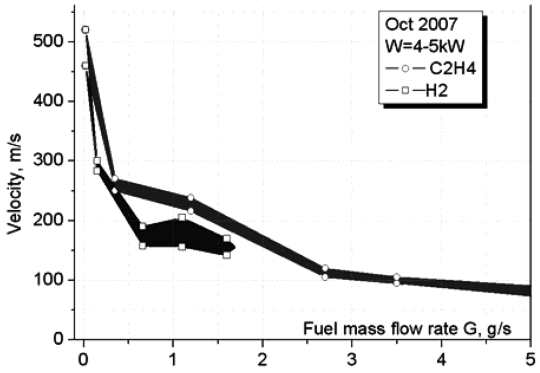

Fig. 10 Dependence of flow velocity within the combustion zone on fuel mass flow rate.

combustion efficiency, this was estimated by the pressure rise and corroborated by chemical analysis of exhaust gases. For both hydrogen and ethylene fueling, combustion efficiency was 70% under optimal conditions. Also, in spite of the "area relief" provided by the inclined bottom wall, thermal choking is observed in the case of hydrogen fueling at $G_{H2} > 1$ g/s.

The next important items are the observation of the flamefront position and measurements of the gas velocity in the combustion zone. These measurements were made by means of the schlieren-streak technique. A schematic of measurements is shown in Fig. 8. Here, a thin laser sheet crosses the flow just above the bottom wall ($Y = 2$ mm) and is affected by density irregularities. The resulting laser sheet intensity pattern is recorded by a fast line scan camera at a frequency of 50 kHz. This technique allows one to obtain a real-time picture of a flow behavior, and a 2-D image of downstream distance and time is created.

Samples of such records are shown in Fig. 9 for hydrogen and ethylene fueling. In the case of ethylene fueling, the luminosity from the discharge increases dramatically, as is seen in Fig. 9 (right), as the fuel and discharge interact. A similar behavior for the flamefront is observed for both hydrogen and ethylene. Ignition occurs several centimeters downstream of the discharge row, and the flamefront appears to move upstream with a velocity that depends on electrical power deposited within the flow and the fuel mass flow rate. After the discharge is switched off, the flame is blown out, as there is no longer a flameholding mechanism. This too can be seen in Fig. 9: near the bottom of both images, subsequent to the discharge switching off, a dark region is seen to be moving rapidly downstream out of the field of view. This method allows one to estimate the physical velocity of the gas as well. The result is shown in Fig. 10. Here, it is seen that the gas flow is subsonic within the region of intense combustion.

The energetic threshold measured for ignition and flameholding by the discharge in this case can be compared with that when employing a cavity and a backward-facing wall step [24,25]. The statistically averaged results are shown in Table 1. In the latter cases, the discharge was configured such that the anode–cathode pair is located with one electrode just upstream and the other just downstream of the step, and this configuration forces the discharge into the cavity (and otherwise it would remain in the shear layer). It can be seen that comparable power levels are required for flameholding with the wall step or on the plane wall. We consider this as a positive result for a practical implementation of this approach of flameholding on a plane wall.

Note that the threshold for flameholding with this configuration does not decrease (improve) as the stagnation temperature T_0 increases from 300 to 650 K, contrary to expectation. The experimental data were analyzed in two cases, constant pressure and constant density, with a similar result. The same effect was found for the wall step configuration and discussed in [25]. Based on results of computational fluid dynamics simulation, the explanation of that behavior was the significant modification of the flow structure in the separation zone and acceleration of the gas exchange within the flameholding region. In the case of the plane wall, a similar idea is taken as a working hypothesis: an increase of the temperature leads to an increase in the gas speed and to a reduction in residence time within the separation zone. So, two main mechanisms can impact the process of ignition and flameholding as the temperature is increased: 1) an acceleration of chemical reactions and 2) a shortening of the residence time. In the range of $T_0 = 300$–650 K, the second process appears dominant here. Finally, one would expect that with further heating of the air, as the autoignition temperature is approached, the plasma power required for ignition and flameholding would decrease; this effect is a key point for further study.

It is seen in Table 1 that a power of several kilowatts is required for ignition and flameholding under our conditions. However, this level is small compared with a typical flow enthalpy of $H = (2$–$4) \times 10^5$ W and a thermal power release due to combustion of $P = (0.2$–$2) \times 10^5$ W. At the same time, a further optimization of a plasma generator may reduce the required power.

Conclusions

We have studied the effects of a transversal discharge on flameholding in a M-2 flow along a plane wall. The main physical effects observed of the plasma on the flowfield are that it heats the gas, generating high concentrations of radicals in the process, and that it modifies the flowfield, potentially inducing separation. The maximum effect at minimal power deposition can be realized with in situ plasma generation, nonequilibrium composition, and a nonuniform discharge structure. Such an approach has been demonstrated in different geometrical configurations (i.e., with a backward-facing step or cavity); however, here the focus was on affecting the flow over a plane wall in a supersonic flow.

Ignition and flameholding were realized for hydrogen and ethylene fueling on a plane wall by using a transversal electrical discharge at relatively low power deposition (2–3% of flow enthalpy). The power threshold for a hydrogen flameholding was measured to be $W_{pl} < 3$ kW. The combustion completeness was estimated to be reasonably high, 70%, with both hydrogen and ethylene fuels under optimal conditions. Thermal choking of the duct was observed at $G_{H2} > 1$ g/s, in spite of the fact that the duct design included an inclined wall for area relief.

The ignition effect of the gas discharge was compared for different levels of discharge power, power density, and reduced electrical field (characterizing the departure from equilibrium for the discharge). Here it was found that the effectiveness of the flameholding is determined primarily by the power deposition and secondarily by the power density. In this experiment the effect of reduced electrical field was not a critically important factor. The power threshold for flameholding with ethylene fueling was measured to be $W_{pl} \geq 4$ kW. In comparison with hydrogen fueling, a main difference with ethylene fueling was that thermal choking was not observed, even at the maximum discharge power of $W_{pl} = 5.6$ kW. Furthermore, the

Table 1 Power threshold of plasma-induced ignition and flameholding of hydrogen (H_2) and ethylene (C_2H_4) in $M = 2$ flow at stagnation temperatures from 300 to 650 K.

Threshold for ignition/flameholding	H_2 ($T_0 = 300$ K)	C_2H_4 ($T_0 = 300$ K)	C_2H_4 ($T_0 = 500$ K)	C_2H_4 ($T_0 = 650$ K)
Ignition in cavity and behind wall step	1 kW	2.5 kW	4 kW	——
Flameholding in shear layer over wall step	<3 kW	3.5 kW	≈5 kW	≈10 kW
Flameholding over plane wall	<3 kW	4.5 kW	>5 kW	>8 kW

completeness of the ethylene combustion decreased with increased fuel mass flow rate.

The position of the flamefront was visualized by a schlieren-streak technique. At a constant fuel flow rate, the flamefront can be controlled by the discharge power in accordance with a qualitative law: higher power = shorter distance between the point of the fuel injection and the flamefront. Another important feature is that "no discharge = no combustion" at all conditions/fuels tested. Moreover, switching off the discharge promptly leads to flame extinction.

Acknowledgments

The experimental work was funded through the European Office of Aerospace Research and Development—International Science and Technology Center Project No. 3057p and by the Russian Academy of Science (Supervisor, Gorimir Cherny).

References

[1] Starikovskaia, S. M., "Plasma Assisted Ignition and Combustion," Topical Review, *Journal of Physics D: Applied Physics*, Vol. 39, No. 16, 2006, pp. R265–R299. doi:10.1088/0022-3727/39/16/R01

[2] Bletzinger, P., Ganguly, B. N., VanWie, D., and Garscadden, A., "Plasmas in High Speed Aerodynamics," Topical Review, *Journal of Physics D: Applied Physics*, Vol. 38, No. 4, 2005, pp. R33–R57. doi:10.1088/0022-3727/38/4/R01

[3] Takita, K., "Ignition and Flameholding by Oxygen, Nitrogen, and Argon Plasma Torches in Supersonic Airflow," *Combustion and Flame*, Vol. 128, No. 3, 2002, pp. 301–313. doi:10.1016/S0010-2180(01)00354-6

[4] Popov, N. A., "The Effect of Nonequilibrium Excitation on the Ignition of Hydrogen-Oxygen Mixtures," *High Temperature*, Vol. 45, No. 2, 2007, pp. 261–279. doi:10.1134/S0018151X07020174

[5] Jacobsen, L. S., Carter, C. D, Baurle, R. A., Jackson, T., Williams, S., Barnett, J., Tam C.-J., Bivolaru, D., and Kuo, S., "Plasma-Assisted Ignition in Scramjets," *Journal of Propulsion and Power*, Vol. 24, No. 4, 2008, pp. 641–654. doi:10.2514/1.27358

[6] Leonov, S. B., Yarantsev, D. A., Napartovich, A. P., and Kochetov, I. V., "Plasma-Assisted Combustion of Gaseous Fuel in Supersonic Duct," *IEEE Transactions on Plasma Science*, Vol. 34, No. 6, 2006, pp. 2514–2525. doi:10.1109/TPS.2006.886089

[7] Klimov, A., Bityurin, V., Brovkin, V., and Leonov, S., "Plasma Generators for Combustion," *Proceedings of the Workshop on Thermo-Chemical Processes in Plasma Aerodynamics*, Joint Institute for High Temperature RAS, 30 May–3 June 2000, p. 74.

[8] Starikovskii, A., "Plasma Supported Combustion," *Proceedings of the Combustion Institute*, Vol. 30, 2005, pp. 2405–2417. doi:10.1016/j.proci.2004.08.272

[9] Starik, A. M., and Titova, N. S., "Low-Temperature Initiation of the Detonation Combustion of Gas Mixtures in a Supersonic Flow Under Excitation of the $O_2(a^1\Delta_g)$ State of Molecular Oxygen," *Doklady Physics*, Vol. 46, No. 9, 2001, pp. 627–632. doi:10.1134/1.1408990 (in Russian).

[10] Kochetov, I. V., Napartovich, A. P., and Leonov, S. B., "Plasma Ignition of Combustion in a Supersonic Flow of Fuel-Air Mixtures: Simulation Problems," *High Energy Chemistry*, Vol. 40, 2006, pp. 98–104. doi:10.1134/S0018143906020068

[11] Morris, R. A., Arnold, S. T., Viggiano, A. A., Maurice, L. Q., Carter, C., and Sutton, E. A., "Investigation of the Effects of Ionization on Hydrocarbon-Air Combustion Chemistry," *2nd Weakly Ionized Gases Workshop Proceedings*, AIAA, Reston, VA, 1998, pp. 163–176.

[12] Brown, M. S., Forlines, R. A., and Ganguly, B. N., "Measurements of CH Density in a Pulsed-dc Hydrocarbon-Gas Mixture Discharge," *Journal of Applied Physics*, Vol. 97, 2005, pp. 103302-1–103302-6. doi:10.1007/10828028_1

[13] Chintala, N., Meyer, R., Hicks, A., Bao, A., Rich, J. W., Lempert, W. R., and Adamovich, I. V., "Nonthermal Ignition of Premixed Hydrocarbon-Air Flows by Nonequilibrium Radio Frequency Plasma," *Journal of Propulsion and Power*, Vol. 21, No. 4, 2005, pp. 583–590. doi:10.2514/1.10865

[14] Esakov, I. I., Grachev, L. P., Khodataev, K. V., Vinogradov, V. A., and Van Wie, D., "Efficiency of Propane-Air Mixture Combustion Assisted by Deeply Undercritical MW Discharge in Cold High-Speed Airflow," AIAA Paper 2006-1212, Jan. 2006.

[15] Kim, W., Do, H., Mungal, M. G., and Cappelli, M. A., "Investigation of NO Production and Flame Structure in Plasma Enhanced Premixed Combustion," *Proceedings of the Combustion Institute*, Vol. 31, 2007, pp. 3319–3326. doi:10.1016/j.proci.2006.07.107

[16] Magre, P., Sabel'nikov, V., Teixeira, D., and Vincent-Randonnier, A., "Effect of a Dielectric Barrier Discharge on the Stabilization of a Methane-Air Diffusion Flame," ISABE Paper 2005-1147, Sept. 2005.

[17] Starikovskaia, S., Kosarev, I., Krasnochub, A., Mintoussov, E., and Starikovskii, A., "Control of Combustion and Ignition of Hydrocarbon-Containing Mixtures by Nanosecond Pulsed Discharges," AIAA Paper 2005-1195, Jan. 2005.

[18] Rosocha, L. A., and Kim, Y., "Effects of Silent Electrical Discharge Excitation on the Combustion of Methane, Propane and Butane," *17th International Symposium on Plasma Chemistry*, Univ. of Toronto Press, Inc., 7–12 Aug. 2005, Topic 13, pp. 1001–1002.

[19] Pilla, G., Galley, D., Lacoste, D. A., Lacas, F., Veynante, D., and Laux, C. O., "Stabilization of a Turbulent Premixed Flame Using a Nanosecond Repetitively Pulsed Plasma," *IEEE Transactions on Plasma Science*, Vol. 34, No. 6, 2006, pp. 2471–2477. doi:10.1109/TPS.2006.886081

[20] Abe, N., Ohashi, R., Takita, K., Masuya, G., and Ju, Y., "Effects of NO_x and HO_2 on Plasma Ignition in a Supersonic Flow," AIAA Paper 2006-7971, Nov. 2006.

[21] Aleksandrov, A., Bychkov, V., Chernikov, V., Ershov, A., Gromov, V., Kolesnikov, E., Levin, V., Shibkov, V., and Vinogradov, V., "Arc Discharge as a Means for Ignition and Combustion of Propane-Air Mixture Supersonic Flow," AIAA Paper 2006-1462, Jan. 2006.

[22] Billingsley, M. C., Sanders, D. D., O'Brien, W. F., and Schetz, J. A., "Improved Plasma Torches for Application in Supersonic Combustion," *13th AIAA/CIRA International Space Planes and Hypersonic Systems and Technologies Conference*, AIAA, Reston, VA, 16–20 May 2005.

[23] Leonov, S., Bityurin, V., Savelkin, K., and Yarantsev, D., "Progress in Investigation for Plasma Control of Duct-Driven Flows," AIAA Paper 2003-0699, Jan. 2003.

[24] Leonov, S., Carter, C., Starodubtsev, M., and Yarantsev, D., "Mechanisms of Fuel Ignition by Electrical Discharge in High-Speed Flow," AIAA Paper 2006-7908, Nov. 2006.

[25] Leonov, S. B., Carter, C., Savelkin, K. V., Sermanov, V. N., and Yarantsev, D. A., "Experiments on Plasma-Assisted Combustion in $M = 2$ Hot Test-Bed PWT-50H," AIAA Paper 2008-1359, Jan. 2008.

[26] Leonov, S., Bityurin, V., and Yarantsev, D., "The Effect of Plasma-Induced Separation," AIAA Paper 2003-3853, June 2003.

C. Segal
Associate Editor